AGU PUBLICATIONS

Geophysical Research Letters

RESEARCH LETTER
10.1002/2014GL060440

Key Points:
- O^+ participates in magnetotail reconnection
- Current sheet thickness scales with H^+ gyroradius
- O^+ has no effect on the thickness

Correspondence to:
Y. H. Liu,
yhliu@atlas.sr.unh.edu

Citation:
Liu, Y. H., L. M. Kistler, C. G. Mouikis, V. Roytershteyn, and H. Karimabadi (2014), The scale of the magnetotail reconnecting current sheet in the presence of O^+, *Geophys. Res. Lett.*, *41*, 4819–4827, doi:10.1002/2014GL060440.

Received 5 MAY 2014
Accepted 3 JUL 2014
Accepted article online 5 JUL 2014
Published online 22 JUL 2014

The scale of the magnetotail reconnecting current sheet in the presence of O^+

Y. H. Liu[1], L. M. Kistler[1], C. G. Mouikis[1], V. Roytershteyn[2], and H. Karimabadi[2]

[1]Space Science Center, Morse Hall, University of New Hampshire, Durham, New Hampshire, USA, [2]SciberQuest, Inc., Del Mar, California, USA

Abstract The reconnection current layer thickness is expected to scale with either the ion inertial length or the ion gyroradius. Both of these quantities scale with the mass of the ions present. During geomagnetically disturbed times, the reconnection layer in the magnetotail can contain a significant amount of O^+. Using Cluster multi-spacecraft measurements, we have studied nine reconnection events in the magnetotail plasmasheet, to determine whether the reconnecting current sheet thickness scales with the ion gyroradius or the ion inertial length, and whether the amount of O^+ in the plasma sheet has an effect on the current layer thickness. We find that the thickness is equal to the H^+ gyroradius, even when the plasma sheet has a high O^+ content. This result is in contrast to Hall MHD expectations and likely results from the multiscale nature of the current sheet.

1. Introduction

One key question in magnetic reconnection is what determines the structure of the reconnection layer. Two-fluid analysis shows that the ions and electrons can move independent of each other at the reconnection site and form a multilayer diffusion region: a smaller electron diffusion region embedded within a larger ion diffusion region [*Sonnerup*, 1979; *Biskamp et al*., 1997]. The scale of electron and ion diffusion regions and the thickness of their associated current layers are about the scale of the electron/ion inertial length or the gyroradius [*Sonnerup*, 1979]. In the generalized Ohm's law, the ion inertial length is introduced via the Hall current, and the ion gyroradius scale is introduced via the ion off-diagonal pressure tensors [*Sonnerup*, 1979]. *Wu et al*. [2011], using particle-in-cell (PIC) simulations, determined that the width of the ion diffusion region scales with the upstream ion inertial length but that the ion local meandering radius also scales as the ion inertial length. Thus, they would expect the thickness to scale as the local gyroradius. Previous observations in the earth's magnetopause and magnetotail have shown that the current sheet thickness is of the order of the ion inertial length in individual cases [*Mozer et al*., 2002; *Runov et al*., 2006; *Phan et al*., 2007; *Xiao et al*., 2007]. However, these studies were only determining rough scales and did not distinguish between ion inertial length and ion gyroradius or compare the thickness quantitatively with the gyroradius. Thus, the question of how the reconnecting current sheet thickness relates to the ion inertial length or gyroradius has not been resolved by observation.

During some substorms, especially during storm times, O^+ can be abundant in the near-earth plasma sheet [*Mouikis et al*., 2010]. These heavier O^+ ions can also be involved in the reconnection process. *Kistler et al*. [2005] used Cluster data to show that O^+ ions can carry more than 10% of the reconnecting current. How these heavy ions affect the reconnecting current sheet thickness observationally has never been addressed.

In this paper, we use Cluster data from time periods when Cluster crosses the region close to the X-line, to perform a statistical study. Two questions are addressed: how does the thickness of the reconnecting current sheet scale with the H^+ and O^+ inertial length and gyroradius, and how does the thickness depend on the O^+ content.

2. Observation

2.1. Instrumentation

The CLUSTER satellites crossed the near-earth reconnection X-line many times in the first four tail seasons. The in situ ion data used in this study are from the Composition and Distribution Function (CODIF) sensor of the Cluster ion spectrometry (CIS) instrument [*Rème et al*., 2001] and the magnetometer instrument (Flux Gate Magnetometer (FGM)) [*Balogh et al*., 2001] onboard Cluster. CODIF measures the three-dimensional distribution

functions of the major ion species over the energy per charge range 40–40,000 eV/e. Since we only focus on the diffusion region crossing time, when the bulk velocity is nearly 0, this energy range is expected to include the bulk of the density and pressure in our study.

2.2. Current Sheet Thickness Measurements

The current sheet in the earth's magnetotail can be simply modeled as a one-dimensional Harris Sheet:

$$B_x = B_0 \tanh\left(\frac{z - z_0}{h}\right) \tag{1}$$

, where B_x is the locally measured x component of the magnetic field, B_0 is the lobe field magnitude, z is the spacecraft location, z_0 is the location of the center of the current sheet, and h is the half thickness of the current sheet. The lobe magnetic field, B_0, is estimated from local plasma and magnetic field measurements assuming pressure balance, $B_0 = \sqrt{2\mu P_T}$, where P_T is the averaged total pressure measured by two spacecraft. Thus, there are two unknowns, z_0 and h. Using data measured by two spacecraft, the thickness of the current sheet can be determined by fitting to the 1-D Harris sheet. Since ion data are available from the CODIF instrument on Cluster SC 1, 3, and 4, we can perform up to three estimations of the half thickness of the current sheet if all three spacecraft have measurements during the given time interval. In this study, if one of the spacecraft is located within the lobe, the atanh function is unsolvable, and no thickness is determined.

Another way to estimate the current sheet thickness is using a time-varying Harris sheet fit, as first proposed by *Lui* [1993]. The time-varying Harris current sheet model fitting assumes that:

$$h(t) = \frac{B_0^2(t) - B_x^2(t)}{\mu_0 B_0 J_y(t)}, \tag{2}$$

where all the terms are the same as equation (1) but J_y is calculated via the Cluster four spacecraft curlometer technique [*Dunlop et al*., 2002; *Thompson et al*., 2005]. When the spacecraft separation is smaller than or comparable to the measured current sheet thickness, the curlometer technique is more accurate for estimating the current density and hence the time-varying current sheet thickness than the 2-spacecraft fit.

A third method is to use the magnetic field gradient estimation, a method first proposed by *Shen et al*. [2008]. With the Cluster curlometer technique, we are able to estimate the ∇B during the current sheet crossing. Thus, the half thickness of the current sheet can be expressed as

$$h = \int_0^h dz = \int_{B_{\min}}^{B_0} dB \Big/ |\nabla B| \approx (B_0 - B_{\min}) / \langle |\nabla B| \rangle \tag{3}$$

, where the $B_{\min}$ is the minimum magnitude of the magnetic field during the crossing of current sheet. In this paper, we assume that $B_{\min} \ll B_0$ and get $h = B_0/\langle|\nabla B|\rangle$. This method does not assume a Harris sheet model.

2.3. Data

2.3.1. Event Study

We first present the data for one reconnection X-line crossing event. Using this event as an example, we show how the events for the statistical study are selected and how the following parameters are deduced: the reconnecting current sheet thickness h, the H^+ and O^+ gyroradii, ρ_{H^+}, ρ_{O^+}, the H^+ and O^+ inertial length d_{H^+}, d_{O^+}, and the current sheet O^+ to H^+ density ratio n_{O^+}/n_{H^+}. Then we will present the statistical results based on our nine event pool.

Figures 1a–1c show the relative locations of the four Cluster spacecraft during the time interval 15 September 2001/05:02:00UT–15 September 2001/05:06:00UT. The spacecraft have an average separation of ~1000 km. This separation approaches the scale of the reconnecting current sheet thickness and makes the implementation of the curlometer technique possible. In Figure 2, we present data measured by the Cluster spacecraft during this interval. Cluster SC4 crosses the current sheet from the north lobe to the south as indicated by the change in Bx in Figure 2d. During the time interval marked by the blue shaded area (around 05:03:30 UT), Cluster SC 1, 3, and 4 observed the H^+ fast flow reversal from earthward to tailward (Figure 2c). Meanwhile, the correlated v_x and B_z reversal (Figures 2c and 2d) and the corresponding Hall field change (Figure 2e) were also observed. These observables have been reported by previous studies [*Birn et al*., 2001; *Eastwood et al*., 2010] and are regarded as the signatures of an X-line crossing. By comparing the theoretical prediction with observed data, the spacecraft

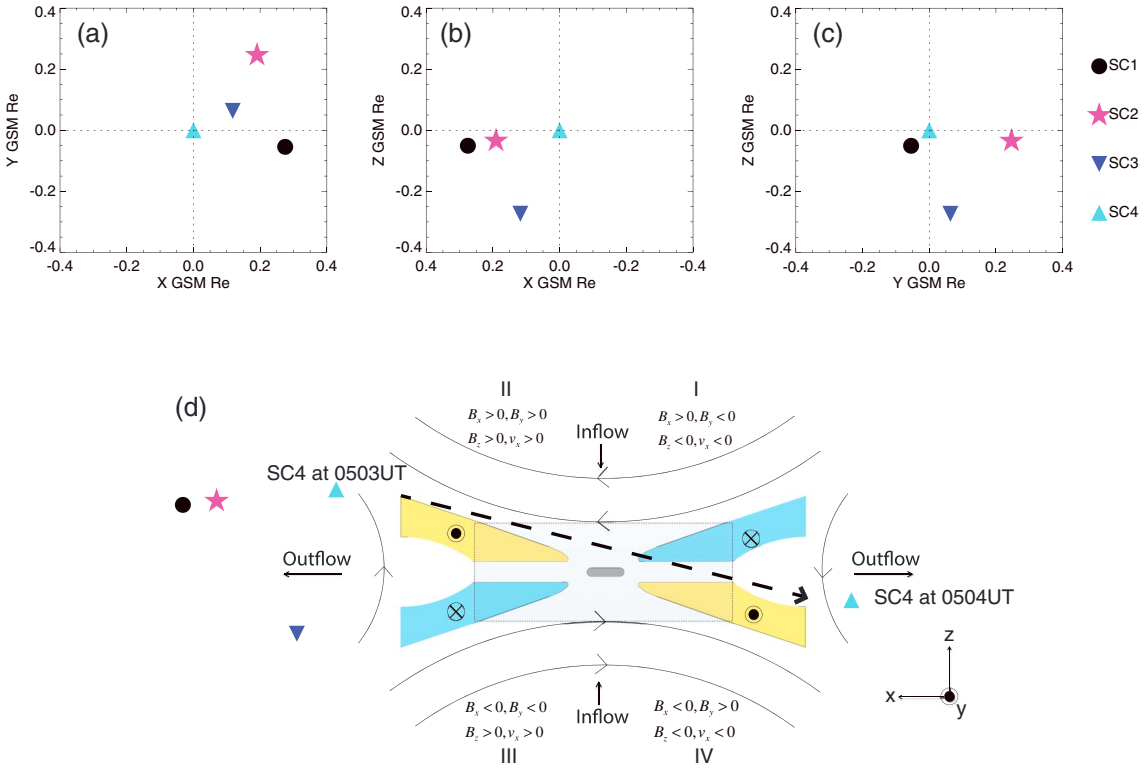

Figure 1. Cluster SC 1, 2, 3, and 4 locations with SC4 as the reference spacecraft in GSM coordinates, projected on (a) XY plane, (b) XZ plane, and (c) YZ plane. Figure 1d shows the SC4 relative locations during its passage of the X-line.

locations relative to the X-line are determined and illustrated in Figure 1d. In addition, we have checked the oxygen distribution functions during the time periods of interest. The purpose of this is twofold: (1) to confirm that Cluster has crossed the X-line in the vicinity of the ion diffusion region; (2) to check whether O^+ has mediated the reconnection process. After 05:03:40UT, SC 1, 3, and 4 entered the earthward outflow region. During the transient time interval 05:03:24UT–05:03:40UT, the fast v_x and B_z reversals are observed. This confirms that this X-line crossing is within the ion diffusion region. In Figure 3, we show the O^+ 2D cuts of the 3D distribution functions measured by SC 1, 3, and 4 in GSM coordinates during the identified transient interval. The $v_x - v_y$ cuts (first column) show that the O^+ ions move in the $+v_y$ direction, at the locations of all three spacecraft. The $v_x - v_z$ cuts (second column) show that they exhibit counter-streaming beams along the v_z axis. This bouncing motion, while streaming in y, can also be observed in $v_y - v_z$ cut, in the third column. The distribution measured by SC1 shows a shift in $+v_x$ in $v_x - v_y$ and $v_x - v_z$ cuts, compared with SC3 and SC4 measured distributions. Because SC1 is located earthward or downstream from SC3 and SC4 (Figure 1), the shift in $+v_x$ indicates that the O^+ ions have gained an outflow velocity along v_x. The distribution function pattern depicted in Figures 3a–3c demonstrates the classical meandering or Speiser-like orbit of O^+ ions, which shows that O^+ ions are demagnetized and exhibit the signature expected in an active reconnection site. Such a distribution pattern has been discussed by *Hoshino et al.* [1998] within the ion diffusion region and is different from the distribution in the initial Harris sheet. The distributions in the initial Harris sheet, both in simulations and in our observations, consist of meandering particles with a broad range of thermal velocities in the hot plasmas forming a Maxwellian. In Figure 3d, we show such an example of the Maxwellian-like O^+ distribution function around central current sheet during geomagnetically quiet time. Using the distribution function as a diagnostic, we can confirm that O^+ is involved in the reconnection process and that the spacecraft crossed the O^+ diffusion region.

After performing the checks stated above, we collect the parameters to prepare for the statistical study. The dashed vertical line in Figure 2 marks the SC4 v_x and B_z reversal time, which is around the 05:03:35UT. At this time, the y component of the current density j_s (Figure 2g) is the dominant component, and $|\nabla \cdot B|/|\nabla B|$

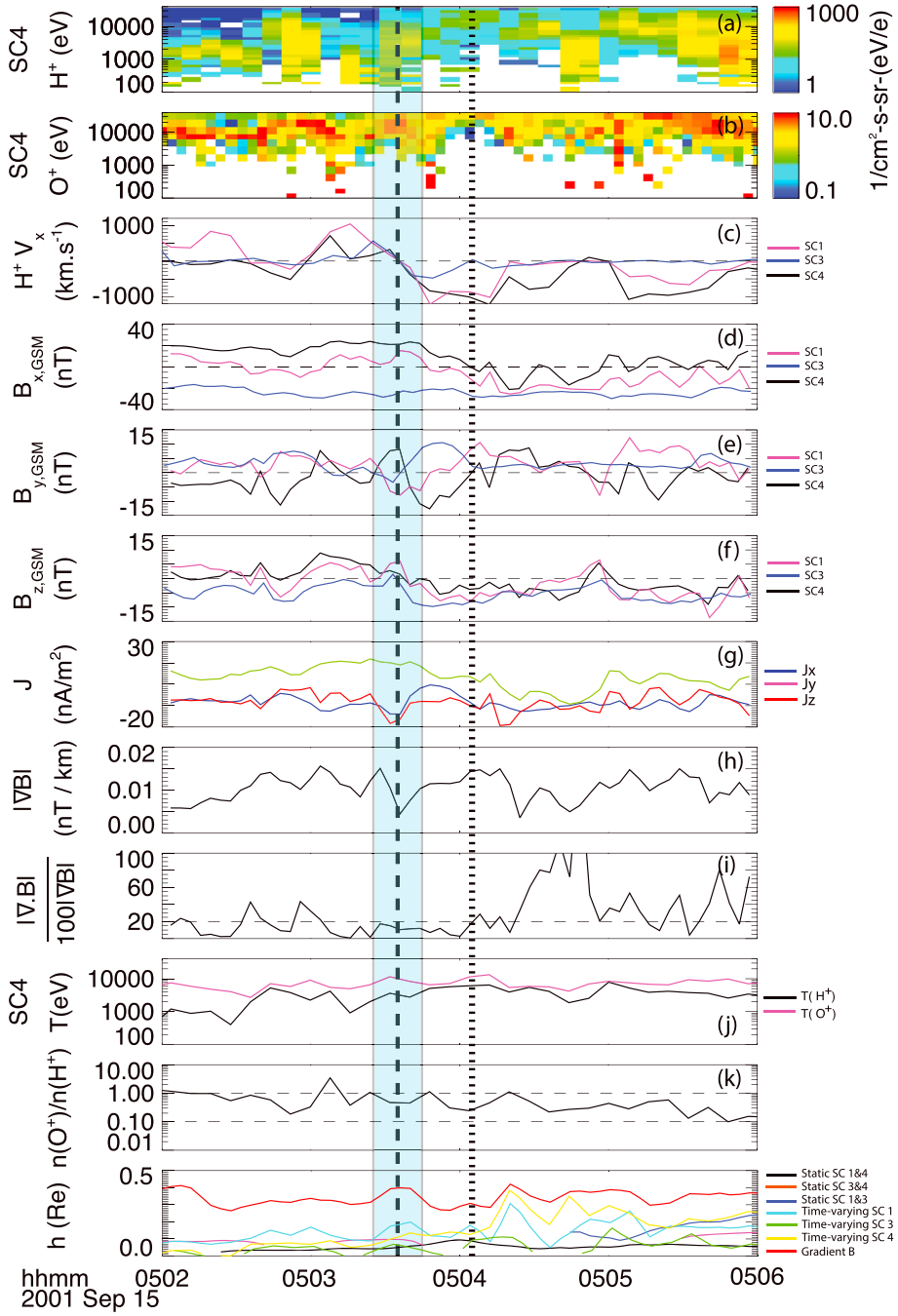

Figure 2. Data from a Cluster diffusion region crossing on 15 September 2001 from 0502 to 0506. (a) The SC4 measured H^+ differential flux versus energy and time, (b) O^+ differential flux versus energy and time, (c) x component of H^+ velocity, on SC 1, 3, and 4, (d) GSM Bx on SC 1, 3, and 4, (e) GSM By on SC 1, 3, and 4, (f) GSM Bz on SC 1, 3, and 4, (g) current density, (h) $|\nabla B|$, (i) percentage of $|\nabla \cdot B|$ over $|\nabla B|$, (j) H^+ and O^+ temperature, from SC4, (k) H^+ to O^+ density ratio from SC4, and (l) estimated half current sheet thickness by different methods. The first vertical line marks the SC4 measured correlated v_x and B_z reversal time, and the second vertical line marks when SC4 crossed the central current sheet ($B_x = 0$).

(Figure 2i) is below 0.2, indicating that the curlometer technique is applicable [*Dunlop et al.*, 2002]. Hence, the j_y and $|\nabla B|$ are both used to calculate the current sheet thickness. Figure 2l shows the half current sheet thickness calculated via all methods: the static Harris sheet fitting for the three spacecraft pairs, the time-varying Harris sheet fitting for each spacecraft, and the gradient B estimation methods. All estimates are

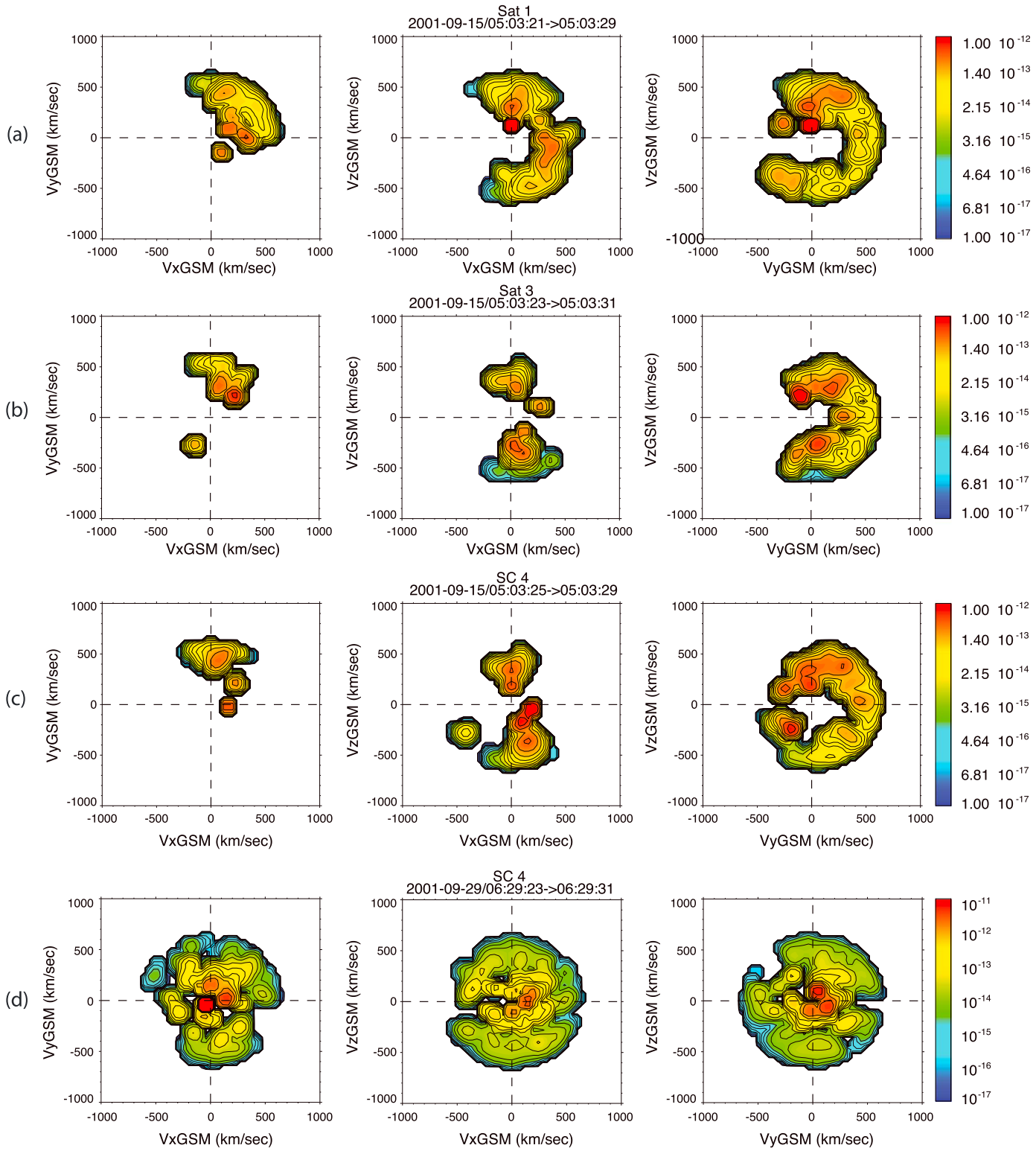

Figure 3. O^+ 3D distribution function measured by Composition and Distribution Function (CODIF) onboard (a) SC 1, (b) SC3, (c) SC4 around the diffusion region crossing time, and (d) SC4 in the central current sheet during quiet time.

Table 1. The Identified Reconnection Diffusion Region Crossings in 2001 and 2003 and the In Situ Measured n_{O^+}/n_{H^+} Density

Event	Date	Start	End	$n(O^+)/n(H^+)$
1	2001/08/22	09:40:00	09:45:00	0.021
2	2001/09/10	07:55:00	08:00:00	0.016
3	2001/09/12	13:10:00	13:15:00	0.767
4	2001/09/15	05:00:00	05:05:00	0.336
5	2001/10/01	09:44:00	09:51:00	3.556
6	2001/10/08	12:50:00	13:00:00	0.281
7	2003/09/19	23:28:00	23:33:00	0.081
8	2003/10/04	06:18:00	06:23:00	0.061
9	2003/10/09	02:20:00	02:30:00	0.082

smoothed using a box car algorithm for 30 s. Although the current sheet half thickness as estimated by the different methods varies, the estimations show the same trends in particular around the time of the fast flow reversal. Although the thickness estimation by the gradient method deviates substantially from others in this event, it agrees well with other estimations in other events and excluding this method entirely does not substantially change our statistical result below. Using the identified diffusion region crossing time, shaded blue in Figure 2, we record the values of the local magnetic field magnitude B_T from all spacecraft, the lobe magnetic field magnitude B_0 (not shown), the H^+ and O^+ temperature T_{H+} and T_{O+} (Figure 2j), and the half current sheet thickness from all the estimation methods (Figure 2l). The second dotted vertical line marks the crossing of the center of the current sheet which is identified as the time when B_x is 0 nT by SC4. We use this time to get the ion density n_{H+} and n_{O+} at the center of the current sheet in order to calculate the n_{O+}/n_{H+} density ratio (Figure 2k) and the ion inertial length d_{H+} and $d_{O+}\left(d_s = c/(4\pi n_s e^2/m)^{1/2}\right)$. The average ion gyroradius ρ_{H^+} and $\rho_{O^+}\left(\rho_s = (2T_s m_s)^{1/2}/eB\right)$ can be estimated based on the measured local magnetic field magnitude B_T or asymptotic lobe field B_0 and the temperature T_{H^+} and T_{O^+} around the X-line crossing time (B_T, B_0, T_{H^+}, and T_{O^+} are recorded at the first dashed line Figure 2). For consistency, we only use the ion composition and temperature measured by SC4 in our statistical study. However, for the local magnetic field, we use the measurements for all spacecraft that are in the diffusion region.

2.3.1. Statistical Study

For our statistical study we refined the event pool of X-line crossings observed by Cluster as reported in *Eastwood et al.* [2010]. *Eastwood et al.* [2010] provided a list of 19 Cluster X-line crossings with one guide field case and 18 antiparallel cases, mainly identified using the v_x and B_z reversal criterion. Some of these crossings are very close to each other, so we first combined crossings from similar times as representing one event to make each selected event unique. The crossings in 2002 are not used because the large spacecraft separation (4000 km) cannot be used to implement the curlometer technique. In addition, both the e^- and O^+ distribution functions are checked to confirm the crossing of the ion diffusion region and the O^+ involvement in the reconnection process. After this filtering we are left with nine events from 2001 and 2003. The spacecraft separation is 1000 km in 2001 and 300 km in 2003, and all these nine events show the signatures of the ion diffusion region crossing according to our criteria. For each of these events the statistical parameters are collected, as our previous example illustrated. In Table 1, we list the events and the in situ measured n_{O+}/n_{H+} density ratio. The value of n_{O+}/n_{H+} is widely distributed and can be used as a parameter to evaluate the O^+ effect on current sheet thickness.

Figure 4 shows the statistical results. Each data point represents one event. In Figures 4a and 4b, we show the reconnecting current sheet half thickness as a function of the H^+ and O^+ gyroradius calculated using the local magnetic field B_T. Each point represents the median value of at least five and at most seven estimations of the current sheet half thickness, using the 1-D Harris fit (up to three estimates), the time-varying Harris sheet method (up to three measurements), and the gradient-B method (one estimate). The vertical error bar gives the range of estimated values. In a few events, the error bar is large due to the disagreements between the estimations from different methods. The horizontal error bars give the range of gyroradii determined using the magnetic field of all spacecraft that are in the diffusion region during the crossing, but not exactly at the neutral sheet. The slopes of the best-fit lines are $h/\rho_{H^+} = 0.91$ and $h/\rho_{O^+} = 0.23$, indicating that the

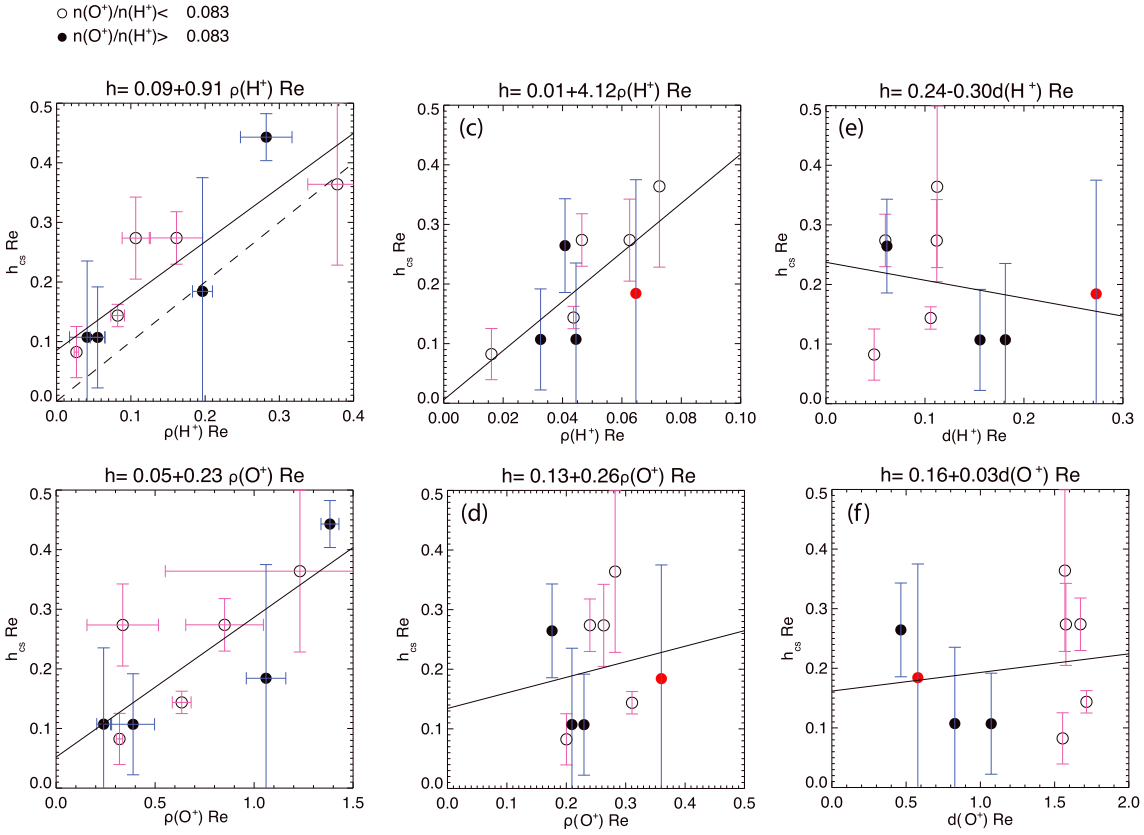

Figure 4. The half current sheet thickness as the function of (a) H^+ gyroradius and (b) O^+ gyroradius estimated with the local magnetic field, (c) H^+ gyroradius and (d) O^+ gyroradius estimated with the lobe magnetic field, and (e) H^+ inertial length and (f) O^+ inertial length estimated with central current sheet plasma density. Each point represents the median value of multiple measurements and the error bar is the median absolute deviation. The filled circles indicate higher O^+ to H^+ density ratio, and open circles indicate lower O^+ to H^+ density ratio. The circle filled with red marks the 1 October 2001 event which has an extremely high O^+ to H^+ density ratio.

current sheet half thickness is of the order of the H^+ gyroradious. In addition, the events are separated into low O^+ content events (open circles) and high O^+ content events (filled circles). For this distinction the medium value, 0.082, of the n_{O+}/n_{H+} density ratios listed in Table 1 was used as the threshold. As illustrated, the high O^+ points are randomly dispersed along the same line. The dependence of the current sheet thickness on the H^+ gyroradius is the same, even when the n_{O+}/n_{H+} ratio is high.

Figures 4c and 4d show the correlation between the half current sheet thickness and the ion gyroradius estimated using the lobe magnetic field B_0. Because the variation in the lobe field determined for the three spacecraft is small, no horizontal error bar is included. There is a correlation of the current sheet thickness with the lobe H^+ gyroradius, with a slope corresponding to 4.12 times the lobe H^+ gyroradius. The correlation of the thickness with the H^+ gyroradius is weak. Figures 4e and 4f show the correlation of the half current sheet thickness with the local ion inertial length for H^+ and O^+. No obvious correlation with the current sheet thickness is observed. Since it is not possible to estimate the lobe densities from the local plasma sheet measurements, no comparison can be made between the current sheet thickness and the lobe ion inertial length.

3. Discussion

Our results indicate that the reconnecting current sheet half thickness is about the scale of H^+ gyroradius, independent of the O^+ abundance, rather than being a hybrid of the two values. However, we show that O^+ does become involved in the reconnection process. The O^+ distribution function pattern indicating that O^+ ions perform a meandering motion across the tail is observed and is used as another signature to identify the ion diffusion region crossing.

Some insight into this result comes from a comparison with the results of *Artemyev et al*. [2008]. *Artemyev et al*. [2008] used Cluster data to study the thickness of thin current sheets and found that the current sheet thickness is wider when there is more O^+ content. This study did not focus specifically on reconnection events. In *Artemyev et al*. [2008], they used a non-Harris sheet model developed by *Zelenyi et al*. [2006] to fit the current sheet. In this model, a flattened tail in the current profile contributed by O^+ has been taken into account, and the flattened tail of the current sheet does get widened by O^+ and reaches the scale of the plasma sheet. In our study, we have used the Harris-type current sheet (static Harris sheet fitting and time-varying Harris sheet fitting), in which the scale of the dramatic change in the current density is defined to be the current sheet thickness. Thus, it may be that the detailed current sheet profile is affected by the O^+, but the largest change in current sheet density is dominated by the H^+ contribution. Thus, it is likely that it is the multiscale structure of the current sheet that leads to the difference between our results and *Artemyev et al*. [2008].

This multiscale structure is expected because the O^+ ions have a larger gyroradius ($\rho_{O^+} = 4\rho_{H^+}$), than the H^+ ions at the same initial energy. Thus, O^+ can be demagnetized earlier than H^+ around the X-line, due to its larger gyroradius, which will result in a wider O^+ diffusion region outside the H^+ diffusion region. Our result shows that the wider O^+ diffusion region does not significantly affect the overall current sheet thickness, which is still dominated by the inner H^+ contribution. In the X-line region, the ions perform a meandering motion, with the particles bouncing in the z direction and drifting in the y direction. Meanwhile, the particle gains energy from its motion along the electric field E_y. However, the acceleration process cannot go infinitely, because the particle will finally become magnetized and be guided by the B_z component to be ejected out in the x direction with fast speed [*Speiser*, 1967; *Hoshino et al*., 1998]. The net motion of ions in the dawn-dusk direction then carries the current. Because the H^+ ions have a lower mass, they can be more easily accelerated in the y direction and reach a higher v_y within the smaller H^+ diffusion region, while O^+ can only reach these velocities downstream of the H^+ diffusion region but in the O^+ diffusion region. This can be compared with the *Shay and Swisdak* [2004] results, where they found that the H^+ reaches a higher outflow speed around the X-line while O^+ reaches its maximum outflow speed further downstream, and with a lower value than the H^+ maximum velocity. Therefore, H^+ is still the main current carrier in the H^+ diffusion region, while O^+ only contributes a small fraction of the current. O^+ may still dominate the current within the O^+ diffusion region, further downstream. In addition, H^+ is the dominant species in all of our events, except the 2001 October 1 event (table 1). The 2001 October 1 event (red filled circle in Figure 4) has an extremely high n_{O+}/n_{H+} ratio, but the estimated thickness is still about the scale of the H^+ gyroradius, although the error bars are large. This might indicate that because the H^+ contribution is more spatially concentrated, it can still control the current sheet thickness even when it is not the dominant ion species. Because the cross-tail velocity of the H^+ ions are higher, the current is mainly carried by H^+, and the dramatic change of current density still occurs on the H^+ scale around the X point. Within the O^+ diffusion region, the current carried by the demagnetized O^+ is much smaller than the bulk current.

In this study, we found that the reconnecting current sheet thickness scales with the ion gyroradius, not with the ion local inertial length. This is consistent with the finding by *Wu et al*. [2011]. As discussed in the introduction, *Wu et al*. [2011] found that the thickness of the current sheet scales with the upstream ion inertial length but that the meandering gyroradius in the current sheet thickness scales as the upstream ion inertial length, as well. Thus, they would expect that the thickness would scale as the local gyroradius.

The result that the current sheet thickness does not vary with the plasma composition may explain the findings by *Liu et al*. [2013], who showed that a higher pre-onset O^+ density in the plasma sheet can result in a faster unloading rate during the substorm expansion phase. The current sheet thickness has a strong controlling influence over the loading and unloading rates during substorms. As shown in *Karimabadi et al*. [2011], the growth rate is an increasing function of ρ/L. If L is determined by H^+ only, independent of composition, then the high O^+ case would approach $\rho/L = 4$ while the low O^+ case has $\rho/L = 1$. This in turn leads to a faster tearing growth rate in the high O^+ case which may result in faster unloading rates [*Karimabadi et al*., 2011] as was found in the Cluster observations by *Liu et al*. [2013].

Acknowledgments
We are grateful to the many engineers and scientists from UNH, MPE, CESR, MPS, IFSI, IRF, UCB, and UW who made the development of the CIS instrument possible. Work at UNH was supported by NASA under grants NNX10AQ42G and NNX11AB65G. The data for this paper are available at Cluster Active Archive System.

The Editor thanks two anonymous reviewers for their assistance in evaluating this paper.

References

Artemyev, A. V., A. A. Petrukovich, L. M. Zelenyi, H. V. Malova, V. Y. Popov, R. Nakamura, A. Runov, and S. Apatenkov (2008), Comparison of multi-point measurements of current sheet structure and analytical models, *Ann. Geophys.*, *26*(9), 2749–2758.

Balogh, A., et al. (2001), The Cluster Magnetic Field Investigation: Overview of in-flight performance and initial results, *Ann. Geophys.*, *19*(10-12), 1207–1217, doi:10.5194/angeo-19-1207-2001.

Birn, J., et al. (2001), Geospace Environmental Modeling (GEM) Magnetic Reconnection Challenge, *J. Geophys. Res.*, *106*(A3), 3715–3719, doi:10.1029/1999JA900449.

Biskamp, D., E. Schwarz, and J. F. Drake (1997), Two-fluid theory of collisionless magnetic reconnection, *Phys. Plasmas*, *4*(4), 1002–1009, doi:10.1063/1.872211.

Dunlop, M. W., A. Balogh, K. H. Glassmeier, and P. Robert (2002), Four-point Cluster application of magnetic field analysis tools: The Curlometer, *J. Geophys. Res.*, *107*(A11), 1384, doi:10.1029/2001JA005088.

Eastwood, J. P., T. D. Phan, M. Oieroset, and M. A. Shay (2010), Average properties of the magnetic reconnection ion diffusion region in the Earth's magnetotail: The 2001- 2005 Cluster observations and comparison with simulations, *J. Geophys. Res.*, *115*, A08215, doi:10.1029/2009JA014962.

Hoshino, M., T. Mukai, T. Yamamoto, and S. Kokubun (1998), Ion dynamics in magnetic reconnection: Comparison between numerical simulation and Geotail observations, *J. Geophys. Res.*, *103*(A3), 4509–4530, doi:10.1029/97JA01785.

Karimabadi, H., V. Roytershteyn, C. G. Mouikis, L. M. Kistler, and W. Daughton (2011), Flushing effect in reconnection: Effects of minority species of oxygen ions, *Planet. Space Sci.*, *59*(7), 526–536, doi:10.1016/j.pss.2010.07.014.

Kistler, L. M., et al. (2005), Contribution of nonadiabatic ions to the cross-tail current in an O^+ dominated thin current sheet, *J. Geophys. Res.*, *110*, A06213, doi:10.1029/2004JA010653.

Liu, Y., L. M. Kistler, C. G. Mouikis, B. Klecker, and I. Dandouras (2013), Heavy ion effects on substorm loading and unloading in the Earth's magnetotail, *J. Geophys. Res.. Space Physics*, *118*, 2101–2112, doi:10.1002/jgra.50240.

Lui, A. T. Y. (1993), Inferring global characteristics of current sheet from local measurements, *J. Geophys. Res.*, *98*(A8), 13,423–13,427, doi:10.1029/93JA01436.

Mouikis, C. G., L. M. Kistler, Y. H. Liu, B. Klecker, A. Korth, and I. Dandouras (2010), H^+ and O^+ content of the plasma sheet at 15–19 Re as a function of geomagnetic and solar activity, *J. Geophys. Res.*, *115*, A00J16, doi:10.1029/2010JA015978.

Mozer, F. S., S. D. Bale, and T. D. Phan (2002), Evidence of diffusion regions at a subsolar magnetopause crossing, *Phys. Rev. Lett.*, *89*(1), doi:10.1103/Physrevlett.89.015002.

Phan, T. D., J. F. Drake, M. A. Shay, F. S. Mozer, and J. P. Eastwood (2007), Evidence for an elongated (>60 ion skin depths) electron diffusion region during fast magnetic reconnection, *Phys. Rev. Lett.*, *99*(25), doi:10.1103/Physrevlett.99.255002.

Rème, H., et al. (2001), First multispacecraft ion measurements in and near the Earth's magnetosphere with the identical Cluster ion spectrometry (CIS) experiment, *Ann. Geophys.*, *19*(10/12), 1303–1354, doi:10.5194/angeo-19-1303-2001.

Runov, A., R. Nakamura, and W. Baumjohann (2006), Multi-point study of the magnetotail current sheet, *Adv. Space Res.Ser.*, *38*(1), 85–92, doi:10.1016/J.Asr.2004.09.024.

Shay, M. A., and M. Swisdak (2004), Three-species collisionless reconnection: Effect of O^+ on magnetotail reconnection, *Phys. Rev. Lett.*, *93*(17), doi:10.1103/PhysRevLett.93.175001.

Shen, C., et al. (2008), Flattened current sheet and its evolution in substorms, *J. Geophys. Res.*, *113*, A07S21, doi:10.1029/2007JA012812.

Sonnerup, B. U. Ö. (1979), Magnetic field reconnection, in *Solar System Plasma Physics*, edited by L. J. Lanzerotti, C. F. Kennel, and E. N. Parker, p. 45, North Holland Publ., Amsterdam.

Speiser, T. W. (1967), Particle trajectories in model current sheets. 2. Applications to auroras using a geomagnetic tail model, *J. Geophys. Res.*, *72*(15), 3919–3932, doi:10.1029/Jz072i015p03919.

Thompson, S. M., M. G. Kivelson, K. K. Khurana, R. L. McPherron, J. M. Weygand, A. Balogh, H. Reme, and L. M. Kistler (2005), Dynamic Harris current sheet thickness from Cluster current density and plasma measurements, *J. Geophys. Res.*, *110*, A02212, doi:10.1029/2004JA010714.

Wu, P., M. A. Shay, T. D. Phan, M. Oieroset, and M. Oka (2011), Effect of inflow density on ion diffusion region of magnetic reconnection: Particle-in-cell simulations, *Phys. Plasmas*, *18*(11), doi:10.1063/1.3641964.

Xiao, C. J., et al. (2007), A Cluster measurement of fast magnetic reconnection in the magnetotail, *Geophys. Res. Lett.*, *34*, L01101, doi:10.1029/2006GL028006.

Zelenyi, L. M., H. V. Malova, V. Y. Popov, D. C. Delcourt, N. Y. Ganushkina, and A. S. Sharma (2006), "Matreshka" model of multilayered current sheet, *Geophys. Res. Lett.*, *33*, L05105, doi:10.1029/2005GL025117.